NEOPLASIA
www.neoplasia.com

Volume 13 Number 3 March 2011 pp. 286–298 286

Astrocytes Upregulate Survival Genes in Tumor Cells and Induce Protection from Chemotherapy[1]

Sun-Jin Kim[*,2], Jang-Seong Kim[*,2], Eun Sung Park[†,2], Ju-Seog Lee[†,2], Qingtang Lin[*], Robert R. Langley[*], Marva Maya[*], Junqin He[*], Seung-Wook Kim[*], Zhang Weihua[*], Krishnakumar Balasubramanian[*], Dominic Fan[*], Gordon B. Mills[†], Mien-Chie Hung[‡] and Isaiah J. Fidler[*]

*Department of Cancer Biology, The University of Texas MD Anderson Cancer Center, Houston, TX, USA; †Department of Systems Biology, The University of Texas MD Anderson Cancer Center, Houston, TX, USA; ‡Department of Molecular and Cellular Oncology, The University of Texas MD Anderson Cancer Center, Houston, TX, USA

Abstract

In the United States, more than 40% of cancer patients develop brain metastasis. The median survival for untreated patients is 1 to 2 months, which may be extended to 6 months with conventional radiotherapy and chemotherapy. The growth and survival of metastasis depend on the interaction of tumor cells with host factors in the organ microenvironment. Brain metastases are surrounded and infiltrated by activated astrocytes and are highly resistant to chemotherapy. We report here that coculture of human breast cancer cells or lung cancer cells with murine astrocytes (but not murine fibroblasts) led to the up-regulation of survival genes, including *GSTA5*, *BCL2L1*, and *TWIST1*, in the tumor cells. The degree of up-regulation directly correlated with increased resistance to all tested chemotherapeutic agents. We further show that the up-regulation of the survival genes and consequent resistance are dependent on the direct contact between the astrocytes and tumor cells through gap junctions and are therefore transient. Knocking down these genes with specific small interfering RNA rendered the tumor cells sensitive to chemotherapeutic agents. These data clearly demonstrate that host cells in the microenvironment influence the biologic behavior of tumor cells and reinforce the contention that the organ microenvironment must be taken into consideration during the design of therapy.

Neoplasia (2011) 13, 286–298

Introduction

In the United States, more than 40% of cancer patients develop brain metastasis; specifically, nearly 50% of patients with lung cancer, 25% of patients with breast cancer, and 15% of patients with melanoma [1–4]. With improved local control and therapy for metastasis to visceral organs, the morbidity and mortality due to late-diagnosed brain metastasis are projected to rise [1,4]. The median survival for untreated patients is 1 to 2 months, which may be extended to 6 months with conventional radiotherapy and chemotherapy [1,4].

The resistance of tumor cells growing in the brain parenchyma to chemotherapy has been attributed to the inability of circulating chemotherapeutic drugs to penetrate the blood-brain barrier (BBB), which is composed of brain endothelial cells with tight junctions enwrapped with basement membrane, pericytes, and the end-feet

Abbreviations: BBB, blood-brain barrier; CBX, carbenoxolone disodium salt; CMEM, complete Eagle minimum essential medium; GFAP, glial fibrillary acidic protein; GJC, gap junction channel; *GSTA5*, glutathione *S*-transferase A5

Address all correspondence to: Isaiah J. Fidler, DVM, PhD, Cancer Metastasis Research Center, Department of Cancer Biology, The University of Texas MD Anderson Cancer Center, 1515 Holcombe Blvd, Unit 854, Houston, TX 77030.
E-mail: ifidler@mdanderson.org

[1]This work was supported in part by Cancer Center Support grant CA16672 and grants 1U54CA143834-01 (I.J.F.) and CA99031 (G.B.M.) from the National Cancer Institute, National Institutes of Health, and by funds from The Farmer Foundation, Polo on the Prairie, and the Vivian L. Smith Foundation.

[2]Equal first authorship.

Received 5 January 2011; Revised 24 January 2011; Accepted 27 January 2011

DOI 10.1593/neo.11112

of astrocytes [5,6]. Recent data, however, revealed that tumor cells growing in the brain parenchyma release vascular endothelial growth factor and other cytokines that lead to increased vessel permeability [7–9]. Taken together with clinical observations that brain metastases in patients are often diagnosed as lesions surrounded by edema and exhibit leakiness of contrast material, these data rule out the BBB as a sole mechanism of drug resistance. Overexpression of P-glycoprotein by tumor cells growing in the brain microenvironment [10] has also been implicated in tumor cell resistance to chemotherapy. Clinical trials using inhibitors of P-glycoprotein expression, however, failed to reverse the resistance of tumor cells to chemotherapeutic drugs or increase the response rate [1]. Collectively, these data raise the possibility that alternate as-yet-unidentified mechanisms underlie the drug resistance of brain metastasis.

The outcome of metastasis in general and brain metastasis in particular depends on the interaction of specific metastatic cells with host factors in the microenvironment [11]. Histologic examinations of clinical specimens of human brain metastases and experimental murine brain metastases reveal that the lesions are surrounded and infiltrated by reactivated astrocytes that express glial fibrillary acidic protein (GFAP) (Figure 1*A*). Astrocytes contribute to cerebral homeostasis by supporting the BBB [5,12], modulating cerebral blood flow [13,14], regulating the response of the central nervous system to inflammation, and participating in synaptic transmission [15], cytosolic calcium–mediated astrocytic-neuronal signaling [16], and neurovascular coupling [17]. Astrocytes have also been shown to control extracellular homeostasis, such as ion concentration, glucose level, acid-base balance, and supply of metabolic substances to neurons [14,18]. Astrocytes also support immune defense in the brain and protect neuronal cells from waste products [19,20] and damage from hypoxia [21]. Thus, astrocytes protect neurons from alterations in homeostasis. Because metastases develop when tumor cells exploit or usurp the homeostatic mechanisms of their host [11], we became intrigued by the possibility that tumor cells can exploit the cytoprotective properties of astrocytes for protection from apoptosis induced by chemotherapeutic drugs. We have recently reported that, in culture, reactive mouse astrocytes can protect melanoma cells from chemotherapy by sequestering intracellular calcium through gap junction communication channels. These data suggested that tumor cells growing in the brain could harness the protective effects of reactive astrocytes for their own survival [22].

In the current study, we explored whether a direct contact of tumor cells with astrocytes also increases expression of survival genes in the tumor cells. To test this hypothesis, we evaluated the effect of different chemotherapeutics on tumor cells cultured alone, with astrocytes, or with fibroblasts and assayed gene expression in these tumor cells. We also verified the functional correlation of genes identified with protection of tumor cells from taxol by knocking down genes using small interfering RNA (siRNA). We found that astrocytes (but not fibroblasts) in direct cell-to-cell contact with tumor cells protect the tumor cells from apoptosis induced by different chemotherapeutic drugs and that this protection is directly correlated with the up-regulation of several survival genes in the tumor cells.

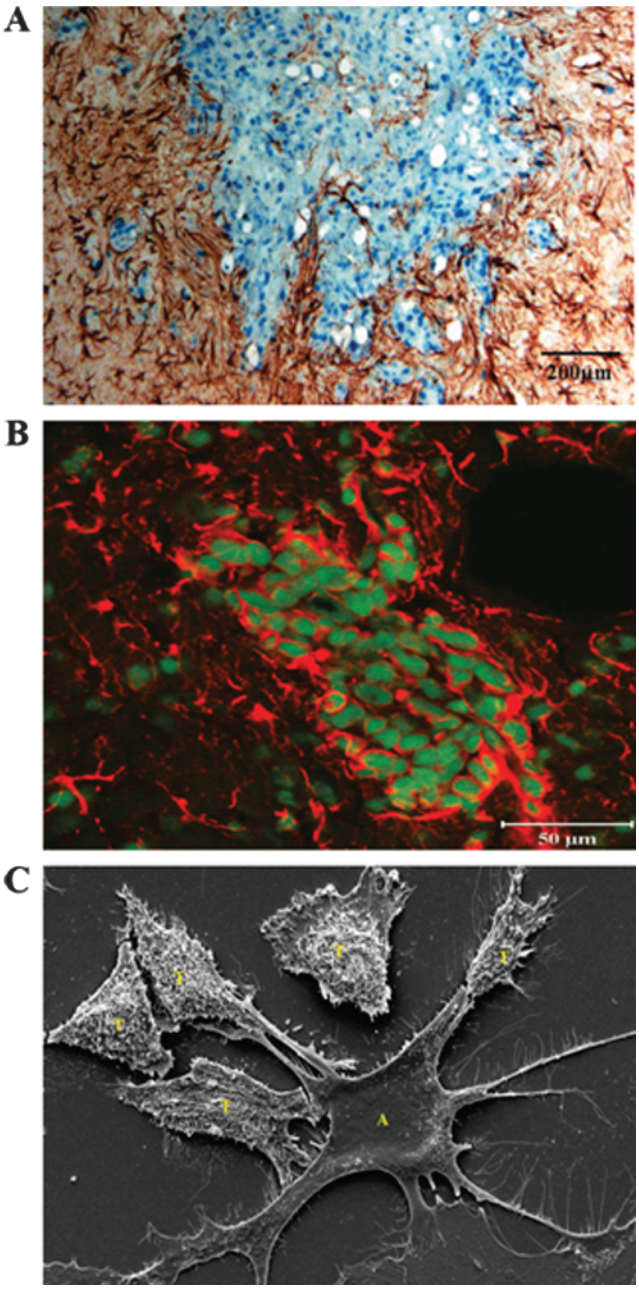

Figure 1. (A) Immunohistochemical analysis of mouse Lewis lung carcinoma (3LL) in the brain of a C57BL/6 mouse. Dividing 3LL cells ($PCNA^+$, blue) are infiltrated and surrounded by activated astrocytes ($GFAP^+$, brown). (B) Immunofluorescent staining of experimental brain metastasis produced by intracarotid injection of human lung adenocarcinoma $PC14Br_4$ cells into nude mouse. Activated astrocytes were stained with GFAP polyclonal antibody (red) and nuclei were stained with SYTOX green. Tumor cells (large nuclei) are surrounded by activated astrocytes. (C) Scanning electron microscopy of *in vitro* culture of human breast cancer MDA-MB-231 cells (T) surrounding a murine astrocyte (A). Note astrocyte end-feet touching tumor cells.

Materials and Methods

Antibodies and Reagents

Antibodies against MAPK, phospho-MAPK (Thr-202 and Tyr-204 phosphorylated), AKT, phospho-AKT (Ser-473 phosphorylated), *TWIST1*, *BCL2L1*, and Myc were purchased from Cell Signaling Technology (Beverly, MA). Glutathione *S*-transferase A5 (*GSTA5*) antibody was purchased from Novus Biologicals (Littleton, CO). β-Actin (cone AC-15) antibody was purchased from Sigma-Aldrich (St Louis, MO), and AKT signal transduction inhibitors (AKT inhibitor,

AKT inhibitor V/Triciribine, and MAPK inhibitors, U0126) were purchased from Calbiochem (San Diego, CA). Carbenoxolone disodium salt (CBX), a gap junction channel (GJC) inhibitor, was purchased from Sigma-Aldrich. All of the chemicals were dissolved in dimethyl sulfoxide, and all other reagents were analytical reagent grade or better.

Immunofluorescent Analysis of Brain Metastasis

Experimental brain metastases were produced by the injection of human lung adenocarcinoma cells $PC14Br_4$ into the internal carotid artery of nude mice [23]. Mice were killed 4 weeks later, and tissue samples were processed in OCT compound for frozen section as previously described [24]. Tissues were sectioned (8-10 μm), mounted on positively charged slides, and air-dried for 30 minutes. Tissue fixation was performed using a protocol consisting of three sequential immersions in ice-cold solutions of acetone, 50:50 (vol/vol) acetone-chloroform, and acetone (5 minutes each). Samples were then washed three times with phosphate-buffered saline (PBS), incubated with protein-blocking solution containing 5% normal horse serum and 1% normal goat serum in PBS for 20 minutes at room temperature, and then incubated with a 1:400 dilution of rabbit anti-GFAP polyclonal antibody (Biocare Medical, Concord, CA) for 18 hours at 4°C. The samples were rinsed four times with PBS for 3 minutes each and then incubated for 1 hour with a 1:1500 dilution of goat antirabbit Cy5 antibody (Jackson ImmunoResearch Laboratories, West Grove, PA). Control samples were labeled with an identical concentration of isotype control antibody and goat antirabbit Cy5 antibody. All samples were rinsed and then briefly incubated with SYTOX green nucleic acid stain (Eugene, OR). The slides were mounted with a glycerol/PBS solution containing 0.1 M propyl gallate (Sigma) to minimize fluorescent bleaching. Confocal images were collected on a Zeiss LSM 510 laser scanning microscope system (Carl Zeiss, Inc, Thornwood, NY) equipped with a motorized Axioplan microscope, argon laser, HeNe laser, LSM 510 control and image acquisition software, and appropriate filters (Chroma Technology Corp, Brattleboro, VT). Composite images were assembled with Photoshop software (Adobe Systems, Inc, Mountain View, CA).

Frozen sections of clinical specimens of metastatic lung cancer to the brain and breast cancer to the brain and lung were processed as described above. Slides were hybridized with rabbit polyclonal antibody against *BCL2L1* (1:200; Cell Signaling), rabbit polyclonal antibody against *TWIST1* (1:200; Cell Signaling), or mouse monoclonal antibody against *GSTA5* (1:200; Novus Biologicals). Fluorescein isothiocyanate–conjugated goat antimouse immunoglobulin G (1:800; Jackson ImmunoResearch Laboratories, Inc) or Alexa Fluor 488 goat antirabbit immunoglobulin G (1:800; Molecular Probes, Carlsbad, CA) were used for the secondary antibody. Nuclei were visualized with 4′,6-diamidino-2-phenylindole (Vector Laboratories, Inc, Burlingame, CA). Images were captured by an Olympus BX-51 microscope (Olympus Imaging America, Inc, Center Valley, PA) with a DP-72 digital camera.

Immunohistochemical Analyses of Brain Metastasis

Formalin-fixed paraffin sections of experimental metastatic C57BL/6 mouse lung cancer (3LL) cells to the brain were processed for double staining with mouse anti–proliferating cell nuclear antigen (PCNA) clone PC-10 (1:200; DAKO A/S, Copenhagen, Denmark) antibody and rabbit anti-GFAP polyclonal antibody (1:400; Biocare Medical, Concord, CA). PCNA-positive cells were visualized using a Ferangi Blue Chromogen Kit (Biocare Medical) as blue and GFAP-positive cells were detected by stable 3′,3′-diaminobenzidine (Research Genetics, Huntsville, AL) as brown. Images were captured by Olympus BX-51 microscopy with a DP-72 digital camera.

Cell Lines and Culture Conditions

Human breast cancer cell line MDA-MB-231, a brain metastatic variant of human lung adenocarcinoma cell line $PC14Br_4$, and murine NIH 3T3 fibroblasts were maintained as monolayer cultures in a complete Eagle minimum essential medium (CMEM) supplemented with 10% fetal bovine serum (HyClone, Logan, UT), L-glutamine pyruvate, nonessential amino acids, two-fold vitamin solution, and penicillin-streptomycin (GIBCO/Invitrogen, Carlsbad, CA). All reagents used for tissue culture were free of endotoxin as determined by the limulus amebocyte lysate assay (Associate of Cape Cod, Woods Hole, MA), and the cell lines were free of the following murine pathogens: *Mycoplasma* spp, Hantan virus, hepatitis virus, minute virus, adenovirus (MAD1, MAD2), cytomegalovirus, ectromelia virus, lactate dehydrogenase–elevating virus, polyma virus, and Sendai virus (assayed by the Research Animal Diagnostic Laboratory, University of Missouri, Columbia, MO). Cells used in this study were from frozen stock, and all experiments were carried out within 10 *in vitro* passages after thawing.

Isolation and Maintenance of Murine Astrocytes

Murine astrocytes were isolated from neonatal mice homozygous for a temperature-sensitive SV40 large T antigen (*H-2K^b-ts*A58 mice; CBA/ca × C57BL/10 hybrid; Charles River Laboratories, Wilmington, MA) and established in culture in our laboratory as described in detail previously [25].

In Vitro *Coculture Chemoprotection Assay*

To determine whether murine astrocytes can induce resistance of tumor cells to chemotherapeutic agents, we performed several *in vitro* chemoprotection assays. Astrocytes and NIH 3T3 fibroblasts were transfected with GFP genes as previously described [26,27]. Target tumor cells, astrocytes, or 3T3 fibroblasts were harvested from a 60% to 70% confluent culture by a brief (2-minute) exposure to 0.25% trypsin in a 0.1% EDTA/PBS solution. The cells were dislodged by tapping the culture flasks briskly and resuspended in CMEM. The murine astrocytes, 3T3 fibroblasts, and tumor cells were plated alone or as cocultures at a tumor cell/astrocyte/3T3 cell ratio of 1:2 onto each of the 35-mm-diameter well of the sterile six-well tissue culture multiwell dish. The cells were allowed to adhere overnight in a humidified 37°C incubator in an atmosphere of 6.4% CO_2 plus air. The cultures were then washed and incubated with fresh CMEM (negative control) or medium containing various concentrations of taxol (Paclitaxel; NDC 0015-3476-30, Bristol-Myers Squibb, Princeton, NJ) and other chemotherapeutic drugs (see below). After 72 hours, the GFP-labeled astrocytes or NIH 3T3 cells were sorted out, and the apoptotic fraction of tumor cells was determined by propidium iodide (PI) staining and FACS analysis (see below).

To determine whether direct contact between tumor cells and astrocytes (or fibroblasts serving as control) was a prerequisite to produce induction of resistance to chemotherapy, we performed the coculture assay using a Transwell-Boyden Chamber, i.e., plating the human tumor cells in the chamber and the mouse astrocytes (or mouse fibroblasts) in the well. After 72 hours of incubation, the apoptotic index of the tumor cells was determined as described below.

To determine whether the induction of tumor cell resistance to chemotherapy was associated with inhibition of P-glycoprotein, we cultured tumor cells alone or with astrocytes (or control 3T3 fibroblasts) at the 1:2 ratio in medium containing either P-glycoprotein–associated drugs, such as taxol (Bristol-Myers Squibb; 5 ng/ml), adriamycin (Pharmacia and Upjohn, Kalamazoo, MI; 200 ng/ml), vinblastine (Sigma; 3 ng/ml), or vincristine (Sigma; 8 ng/ml); or P-glycoprotein–dissociated chemotherapeutic agents, such as 5-FU (Sigma; 500 ng/ml) or cisplatinum (2.4 μg/ml; SICOR Pharmaceuticals, Inc, Irvine, CA). After 72 hours of incubation, the apoptotic index of the tumor cells was determined as described below.

To determine whether astrocyte-mediated protection of tumor cells occurred through GJC, we carried out the cytotoxicity assay in the presence of CBX, a specific inhibitor of GJCs [28,29]. The tumor cells were pretreated for 2 hours with 100 μM CBX and then cocultured with astrocytes or fibroblasts in the presence or absence of 5 ng/ml taxol. The apoptotic index of tumor cells was determined as described below.

In the last set of *in vitro* studies, we determined whether astrocyte-mediated induction of tumor cell resistance to chemotherapeutic drugs was transient or permanent. Human lung cancer $PC14Br_4$ cells were cocultured with either astrocytes or 3T3 fibroblasts in medium alone or medium containing 5 ng/ml taxol. After 72 hours, the astrocytes or 3T3 cells were separated from tumor cells by FACS, and the apoptotic index of the tumor cells was determined in multiple wells by PI staining as described below. From parallel wells, we harvested surviving tumor cells and replated them on monolayers of astrocytes or 3T3 cells. These cocultures were of tumor cells first cocultured with astrocytes and then with either astrocytes or 3T3 cells or of tumor cells first cultured with 3T3 cells and then with either 3T3 cells or astrocytes. The second round of cocultures then received medium containing 5 ng/ml of taxol. After 72 hours, the apoptotic index of tumor cells was determined by PI staining and FACS analysis as described below.

Preparation for PI Staining and FACS Analysis

The supernatant medium containing floating cells was collected from each dish into a 15-ml conical centrifuge tube. The attached cells were harvested by briefly exposing the cells to 0.25% trypsin in a solution containing 0.1% EDTA/PBS. Cells were combined with the corresponding supernatant. The samples were pelleted by centrifugation at 100*g* for 5 minutes. The pellets were resuspended in 10 ml of Hank's balanced salt solution and further pelleted at 100*g* for 5 minutes. The samples were resuspended by vortexing, and the cells were fixed in 1 ml of 1% paraformaldehyde for 10 minutes at room temperature. The samples were then transferred into polypropylene microcentrifuge tubes, and the fixed cells were washed in 1 ml of PBS and then pelleted at 10,000*g* for 1 minute. The pellets were resuspended by vortexing, and the cells fixed overnight in 1 ml of ethanol at −20°C. The cells were again vortexed and pelleted in a microcentrifuge at 10,000*g* for 1 minute. The samples were again vortexed, and the pellets resuspended and stained in 300 μl of PI (50 μg/ml; Cat. P4864; Sigma) containing RNAse (15 μg/ml; Cat. A7973; Promega, Madison, WI) for 20 to 30 minutes at 37°C. The samples were finally transferred to 5-ml plastic culture tubes for FACS analysis using a Coulter EPICS Cytometer (Beckman Coulter, Inc, Fullerton, CA). The apoptotic index was determined by comparing the apoptotic index of tumor cells/apoptotic index of tumor cells and astrocytes or tumor cells and NIH 3T3 fibroblasts × 100 [30]. Values are the mean ± SD of triplicate experiments, and the figures represent three independent experiments.

MTT Assay

Five thousand MDA-MB-231 cells were mixed with an equal number of astrocytes and seeded in 38-mm^2 wells of flat-bottomed 96-well plates in triplicate and allowed to adhere overnight. The cultures were then washed and refed with medium (negative control) or medium containing various concentrations of vinblastine to include the peak plasma level or the drug at 1 μg/ml. After 96 hours, the antiproliferative activity was determined by the MTT assay [31], which monitors the number of metabolically active cells. After a 2-hour incubation in medium containing 0.42 mg/ml MTT, the cells were lysed in 100 μl of dimethyl sulfoxide. The conversion of MTT to formazan by metabolically active viable cells was monitored by a CERES UV900C 96-well microtiter plate scanner at 570 nm (BioTek Instruments, Inc, Winooski, VT). The absorbance of astrocytes treated with vinblastine was used for background subtraction to derive the survival fraction of the MDA-MB-231 from the cocultured values. Percent cytotoxicity was calculated from the following formula: cytotoxicity (%) = $(1 - A / B) \times 100$, where A is the absorbance of treated cells and B is the absorbance of the control cells.

Scanning Electron Microscope Imaging of Cultured Tumor Cells and Astrocytes

Cocultured tumor cells and astrocytes were imaged by scanning electron microscope as previously described with modifications [32]. Detailed experimental procedure is described in the supplemental experimental procedure.

Communication through GJC

Gap junction communication between recipient tumor cells (MDA-MB-231) and donor cells (astrocytes, 3T3 cells, MDA-MB-231) was analyzed by flow cytometry measuring the transfer of dye. Briefly, recipient cells (300,000 cells per well) were plated into a six-well plate and cultured overnight. At that time, donor cells were labeled for 45 minutes with 1 μg/ml green calcein-AM (Molecular Probes) followed by extensive washing. Donor cells (60,000 cells/well) were cocultured for 5 hours with recipient cells either directly or in a Transwell chamber (Transwell-Boyden Chamber, 0.4-μm pore size; Costar, Corning, NY). Cells were harvested, washed, fixed in ethanol, and analyzed by flow cytometry. Gap junction communication was represented as the percentage of the fluorescein isothiocyanate peak that had shifted [33–36].

Gene Expression Profiles by RNA Microarray Analysis

In the first set of gene expression experiments, MDA-MB-231 or $PC14Br_4$ cells were incubated alone, with murine astrocytes, or with NIH 3T3 fibroblasts in a 35-mm-diameter six-well plate (Cat. 353046; BD Falcon, San Jose, CA). The ratio of tumor cells to murine astrocytes or NIH 3T3 cells was set at 1:2. After 72 hours, GFP-labeled murine astrocytes or fibroblasts were sorted out by FACS, and the tumor cells were processed for microarray analyses. In the second set of experiments, we determined whether the expression of genes associated with tumor cell resistance to chemotherapeutic drugs was dependent on continuous contact with astrocytes. MDA-MB-231 or $PC14Br_4$ cells were cocultured with either murine astrocytes or NIH 3T3 cells for 72 hours. The murine astrocytes or NIH 3T3 cells were sorted

out, and tumor cells were either processed to determine gene expression profiles by microarray analyses or plated for a second round of coculture with either murine astrocytes or fibroblasts. Thus, tumor cells first cultured with murine astrocytes were cocultured again with murine astrocytes or with fibroblasts, and conversely, tumor cells initially cultured with fibroblasts were cocultured again with fibroblasts or astrocytes. After a 72-hour incubation, murine astrocytes or fibroblasts were sorted out, and the tumor cells were processed for microarray analyses.

For microarray analyses, total RNA (500 ng) were used for labeling and hybridization according to the manufacturer's protocols (Illumina, Inc, San Diego, CA) using Illumina's Sentrix human 6-v2 Expression BeadChips. The BeadChips were scanned with Illumina BeadArray Reader (Illumina, Inc). The results of microarray data were extracted with Bead Studio 3.7 (Illumina, Inc.) without any normalization or background subtraction. Gene expression data were normalized using quantile normalization method in LIMMA package in R (www.r-project.org) [37]. The expression level of each gene was transformed into a $\log_2$ before further analysis. To select genes that were differentially expressed in two culture groups, we used a class comparison tool in BRB array tools (v3.6; Biometrics Research Branch, National Cancer Institute, Bethesda, MD) as a method for two-sample *t*-test with the estimation of false discovery rate. To avoid potential false-positive genes because of technical variance, all experiments were carried out in quadruplicate.

Western Blot Analysis

Western blot analysis was used to confirm the results of the microarray. Briefly, whole-cell lysates of FACS-sorted tumor cells were prepared using 1 ml of lysis buffer (10 mM Tris [pH 8.0], 1 mM EDTA, 0.1% SDS, 1% deoxycholate, 1% NP40, 0.14 M NaCl, 1 μg/ml leupeptin, 1 μg/ml aprotinin, and 1 μg/ml pepstatin) containing a protease inhibitor mixture (Roche, Indianapolis, IN). Samples containing equal amounts of protein (30 μg) were separated by electrophoresis on 4% to 12% Nu-PAGE gels (Invitrogen) and transferred to nitrocellulose membranes. After blocking with TBS + 0.1% Tween 20 containing 5% nonfat milk, the membranes were incubated at 4°C overnight with primary antibodies (1:1000). Blots were then exposed to horseradish peroxidase–conjugated secondary antibodies (1:3000) and visualized by the enhanced chemiluminescence system from Amersham (Piscataway, NJ). To ensure equal protein loading, we stripped the blots and reprobed with an anti–β-actin antibody.

Knockdown and Overexpression of BCL2L1, GSTA5, *and* TWIST1

Small interfering RNA. RNA interference was performed on MDA-MB-231 cells by using Lipofectamine 2000 (Invitrogen) following the manufacturer's instructions. For silencing target proteins, SMARTpool-sequenced siRNA targeting *BCL2L1* (NM_001191), *GSTA5* (NM_153699), *TWIST1* (NM_000474), and nonspecific control pool (negative control) were purchased from Dharmacon Research (Lafayette, CO). siRNA oligos were diluted in RNAse-free solution and sorted at −80°C. MDA-MB-231 cells of 50% to 60% confluency were transfected with the final concentration of 100 nM siRNA or the nonspecific control siRNA pool. Knockdown of target proteins was confirmed by Western blot using whole-cell lysates prepared 72 hours after transfection.

Overexpression. Myc-tagged ORF clones of *BCL2L1*, *GSTA5*, and *TWIST1* were purchased from OriGene Technologies (Rockville, MD). MDA-MB-231 cells of 80% to 90% confluency were transfected with 10 μg of plasmid of a single gene or a pool of three genes by using Lipofectamine 2000 (Invitrogen) following the manufacturer's instructions. Ten micrograms of pCMV6 plasmid was used as a negative control. Overexpression of target proteins was confirmed by Western blot at various time points.

For chemoprotection assay, tumor cells transfected with siRNA or Myc-tagged target proteins were harvested 12 hours after transfection. Tumor cells were cultured alone, with GFP-murine astrocytes, or with GFP-3T3 cells for 72 hours. Tumor cells were collected by sorting out GFP-murine astrocytes or GFP-3T3 cells, and then the apoptotic fraction of tumor cells was determined by PI staining and FACS analysis as described in the *In Vitro* Coculture Chemoprotection Assay section.

Western Blot Analysis for Expression of AKT/pAKT and MAPK/pMAPK in Human Breast Cancer Cells and Lung Cancer Cells Cultured Alone or Cocultured with Astrocytes or Fibroblasts

Because expression of *BCL2L1* and *TWIST1* has been reported to be related to activated AKT and MAPK pathways leading to anti-apoptosis and survival of the cells and *GSTA5* was related to drug resistance, Western blot analyses were performed for expression of phosphorylated AKT and phosphorylated MAPK. Tumor cells were cocultured for 72 hours with GFP-labeled astrocytes or fibroblasts. The tumor cells were then collected by FACS. Whole-cell lysates were prepared, and equal amounts of proteins were subjected to Western blot analysis with the indicated antibodies.

Determination of the Role of Survival Genes BCL2L1, GSTA5, *and* TWIST1 *in AKT and MAPK Activation and the Role of AKT and MAPK Activation in the Regulation of* BCL2L1, GSTA5, *and* TWIST1 *Gene Expression*

In the first set of experiments, siRNA of nonspecific (NS-siRNA) and combined siRNA (mixed siRNA) were transfected to MDA-MB-231 and $PC14Br_4$ cells. Twelve hours after the transfection, the tumor cells were cultured alone and cocultured with murine astrocytes or fibroblasts. Whole tumor cell lysates were prepared as described. Proteins were subjected to Western blot analysis with indicated antibodies.

In the second set of experiments, MDA-MB-231 and $PC14Br_4$ cells were preincubated for 2 hours with AKT inhibitor (10 μM AKT inhibitor V/Triciribine) and MAPK inhibitor (10 μM U0126) and then cultured for 72 hours alone or cocultured with murine astrocytes or fibroblasts. Whole-cell lysates of tumor cells were prepared and subjected to Western blot analysis using the indicated antibodies.

Statistical Analysis

The apoptotic index was compared by the Student's *t* test. For statistical analysis of gene expression profiles, the expression level of each gene was transformed into a $\log_2$ before further analysis. Class comparison tool in BRB Array Tools (v3.6; Biometrics Research Branch, National Cancer Institute) for a two-sample *t* test with the estimation of false discovery rate was the method used to determine the statistical significance of differentially expressed genes between tumor cells cocultured with different host cells. Genes for Venn diagram analysis were selected by univariate test (two-sample *t* test) with multivariate permutation test (10,000 random permutations). We applied a cutoff

P value < 0.001 to retain genes whose expressions were significantly different between the two groups of tissues examined.

Results

Astrocyte-Tumor Cell Interactions

As shown in Figure 1*A*, mouse lung cancer (3LL) cells (blue) growing in the brain of syngeneic C57BL/6 mouse are surrounded and infiltrated by GFAP-positive (brown) astrocytes. In Figure 1*B*, $PC14Br_4$ human lung cancer cells (green) growing in the brain of a nude mouse are surrounded and infiltrated by GFAP-positive (red) murine astrocytes. In Figure 1*C*, a scanning electron microscopy of *in vitro* cultured human MDA-MB-231 breast cancer cells (T) and murine astrocytes (A) demonstrates direct contact between the astrocytes (extending end-feet) and tumor cells. As clearly shown, a single astrocyte could be in direct contact with multiple tumor cells. Thus, the astrocyte-tumor interactions are evident from both cell cultures and *in vivo* animal experiments.

Astrocytes Protect Tumor Cells from Toxicity of Chemotherapeutic Drugs

Culturing of human MDA-MB-231 breast cancer cells or human $PC14Br_4$ lung cancer cells with astrocytes (but not 3T3 fibroblasts) reduced the apoptotic index (increased resistance) of tumor cells incubated for 72 hours with taxol (5 ng/ml) by 58.3% ± 8.9% (mean ± SD, $P < .01$) and 61.8% ± 6.7% (mean ± SD, $P < .05$), respectively. When tumor cells and astrocytes were separated by a semipermeable membrane (Transwell-Boyden Chamber, 0.4-μm pore size membrane; Costar), the protective effect was not observed. Coculture of tumor cells with 3T3 fibroblasts did not protect tumor cells from chemotherapy (Figure 2*A*). Similarly, coculture of human tumor cells with fibroblasts isolated from the *H-2k*^{b}*-ts*A58 mouse did not protect the tumor cells from treatment with different chemotherapeutic drugs (data not shown). Thus, we conclude that this reduction was dependent on direct contact between tumor cells and astrocytes.

In the next set of experiments, we ruled out the possibility that the astrocyte-mediated protection of tumor cells from taxol was due to P-glycoprotein. Human lung cancer $PC14Br_4$ cells were cultured alone or with astrocytes (1:2 ratio) for 72 hours in medium containing various chemotherapeutic drugs. The astrocytes protected $PC14Br_4$ cells against chemotherapeutic agents that can be excluded from the cell by P-glycoprotein, such as adriamycin ($P < .05$), taxol ($P < .05$), vinblastine ($P < .01$), and vincristine ($P < .01$), and agents that are unrelated to P-glycoprotein, such as 5-FU ($P < .01$) and cisplatinum ($P < .01$) (Figure 2*B*). Astrocytes protected tumor cells from both types of agents, so we conclude that the protection mechanism was unrelated to P-glycoprotein.

We next evaluated the astrocyte-mediated chemoprotection by another assay, i.e., the MTT assay. Human MDA-MB-231 cells were cocultured with astrocytes in medium containing different concentrations of vinblastine. Here again, the data shown in Figure 2*C* demonstrate significant ($P < .01$) protection of tumor cells by the astrocytes. Together, the results suggest that astrocytes protect tumor cells from cytotoxic killing by chemotherapeutic drugs.

GJC of Astrocytes But Not 3T3 Cells Are Involved in Contact-Mediated Protection of Tumor Cells

GJCs have been shown to be involved in the transmission of apoptotic and survival signals between neighboring cells [36,38]. Transfer of

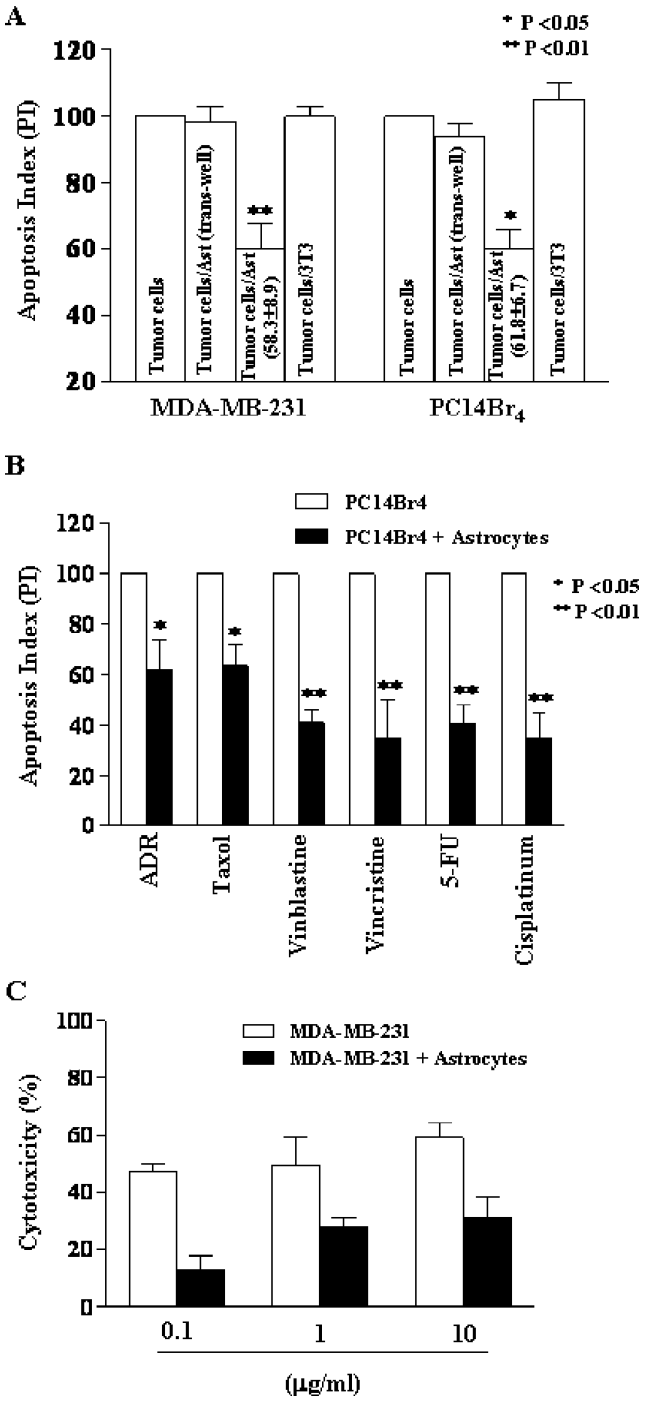

Figure 2. Chemoprotection assay by PI staining and FACS analysis (A, B) or MTT assay (C). (A) Note the significant ($P < .01$) decrease in apoptotic index in tumor cells directly cocultured with astrocytes but not in those cocultured with fibroblasts. Separating the tumor cells from astrocytes with a 0.4-μm pore membrane prevented induction of chemoprotection. (B) Astrocyte-mediated chemoprotection against different chemotherapeutic drugs. Coculture of human lung cancer cell $PC14Br_4$ with astrocytes induced significant protection against all P-glycoprotein–dissociated drugs. (C) Astrocyte protection of tumor cells from vinblastine measured by MTT assay. At various concentrations of vinblastine, coculture of human breast cancer cell MDA-MB-231 with astrocytes induced significant protection ($P < .01$).

the dye clearly occurred between astrocyte-tumor cell cultures in direct contact but did not occur for those cells which were separated by the membrane of the Transwell system (Figure 3*A*).

Similar results were seen for tumor and fibroblast cells or tumor and tumor cells, suggesting that GJCs were able to transfer green calcein-AM dye from donor, including astrocytes, 3T3 cells, or $PC14Br_4$ tumor cells to recipient $PC14Br_4$ tumor cells. To determine whether astrocyte-mediated protection of tumor cells occurred through GJC, we carried out the cytotoxicity assay in the presence of CBX, a specific inhibitor of GJC channels [28,29]. CBX (100 μM) was not toxic to any of the cells tested (data not shown). Control astrocytes, but not fibroblasts, protected the MDA-MB-231 cells (35.5 ± 1.5 *vs* 20.0 ± 3.7, $P < .01$, and 35.5 ± 1.5 *vs* 37.4 ± 0.3, $P > .05$) (Figure 3*B*) and $PC14Br_4$ cells (38.2 ± 0.2 *vs* 20.0 ± 0.8, $P < .01$, and 38.2 ± 0.2 *vs* 34.0 ± 2.1, $P > .05$) (Figure 3*C*) from taxol. However, treatment with CBX completely reversed the protection (33.4 ± 3.3 *vs* 30.8 ± 3.1, $P > .05$ [Figure 3*B*] and 45.3 ± 0.7 *vs* 41.6 ± 0.7, $P > .05$ [Figure 3*C*]). The results suggest that GJCs of astrocytes but not 3T3 cells are involved in contact-mediated protection of tumor cells.

Pattern of Gene Expression in Tumor Cells Cocultured with Astrocytes

To identify cancer cell genes whose expressions were altered only on interaction with astrocytes, human-specific gene expression data from human cancer cells cocultured with murine astrocytes were compared with human-specific gene expression data obtained from cancer cells cocultured with fibroblasts or cultured alone. The data shown in Figure 4*A* demonstrate that human and mouse genes could be clearly differentiated.

Because the coculture of murine astrocytes (but not murine fibroblasts) with tumor cells led to increased resistance of both human breast cancer MDA-MB-231 and human lung cancer $PC14Br_4$ cells to chemotherapy, we sought to identify tumor cell genes whose expressions were commonly altered subsequent to coculture with astrocytes by applying two-sample *t* tests ($P < .001$). Using this procedure, we found that in the MDA-MB-231 cells, 1069 genes, and in the $PC14Br_4$ cells, 594 genes were differentially expressed. A two-gene list comparison revealed increased expression of several genes well known to be associated with drug resistance, antiapoptosis, and survival, such as *GSTA5*, *BCL2L1*, and *TWIST1* (Figure 4*B*). The expression of other multidrug resistance genes or survival genes was not elevated in the described high stringent condition. The expression of these genes was confirmed at the protein level by Western blot analysis of cultured cells (Figure 4*C*) and by immunofluorescent analyses of clinical specimens of breast and lung cancer brain metastases (Figure 4*D*). Examination of clinical specimen of breast cancer metastases to the lung did not reveal expression of *BCL2L1*, *TWIST1*, and *GSTA5* (Figure 4*D*). These data demonstrate the unique feature of the brain microenvironment.

Next, we determined whether the altered gene expression pattern in tumor cells cocultured with astrocytes (but not fibroblasts) was permanent or transient, i.e., is it dependent on a continuous tumor cell contact with astrocytes? The human lung cancer $PC14Br_4$ cells were cocultured for 72 hours with astrocytes or fibroblasts in medium containing taxol (5 ng/ml). Human $PC14Br_4$ lung cancer cells cocultured with astrocytes exhibited a significant decrease in apoptotic index (increased resistance) compared with tumor cells cocultured with fibroblasts (30.9% ± 3.3% and 54.6% ± 0.6%, respectively, $P < .01$). Parallel cultures of tumor cells cocultured with astrocytes or fibroblasts for 72 hours were collected and then reincubated with astrocytes or fibroblasts for another 72 hours in medium containing 5 ng/ml taxol. Tumor cells initially cocultured with astrocytes and again with astrocytes had a significant decrease in apoptotic index compared with tumor

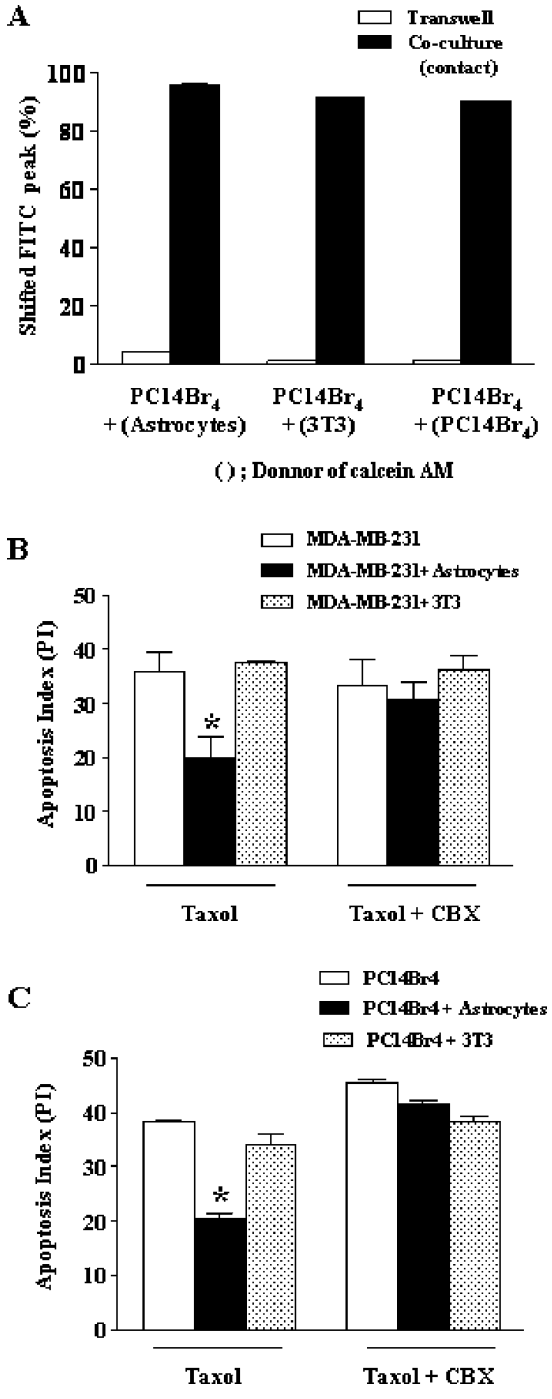

Figure 3. (A) Gap junction assay. Transfer of calcein AM from the donor cells to the recipient cells was observed only when donor cells and recipient cells were cocultured in direct contact. When cells were cultured in Transwell system, which inhibited direct cell contact between donor and recipient cells, gap junction was not established between them, and consequently, calcein AM was not transferred to the donor cells. (B and C) Effect of CBX on chemoprotection. Chemoprotection assay was performed by PI staining and FACS analysis. CBX significantly reversed the protective effects induced by astrocytes in MDA-MB-231 (B) and PC14Br4 (C). *$P < .01$.

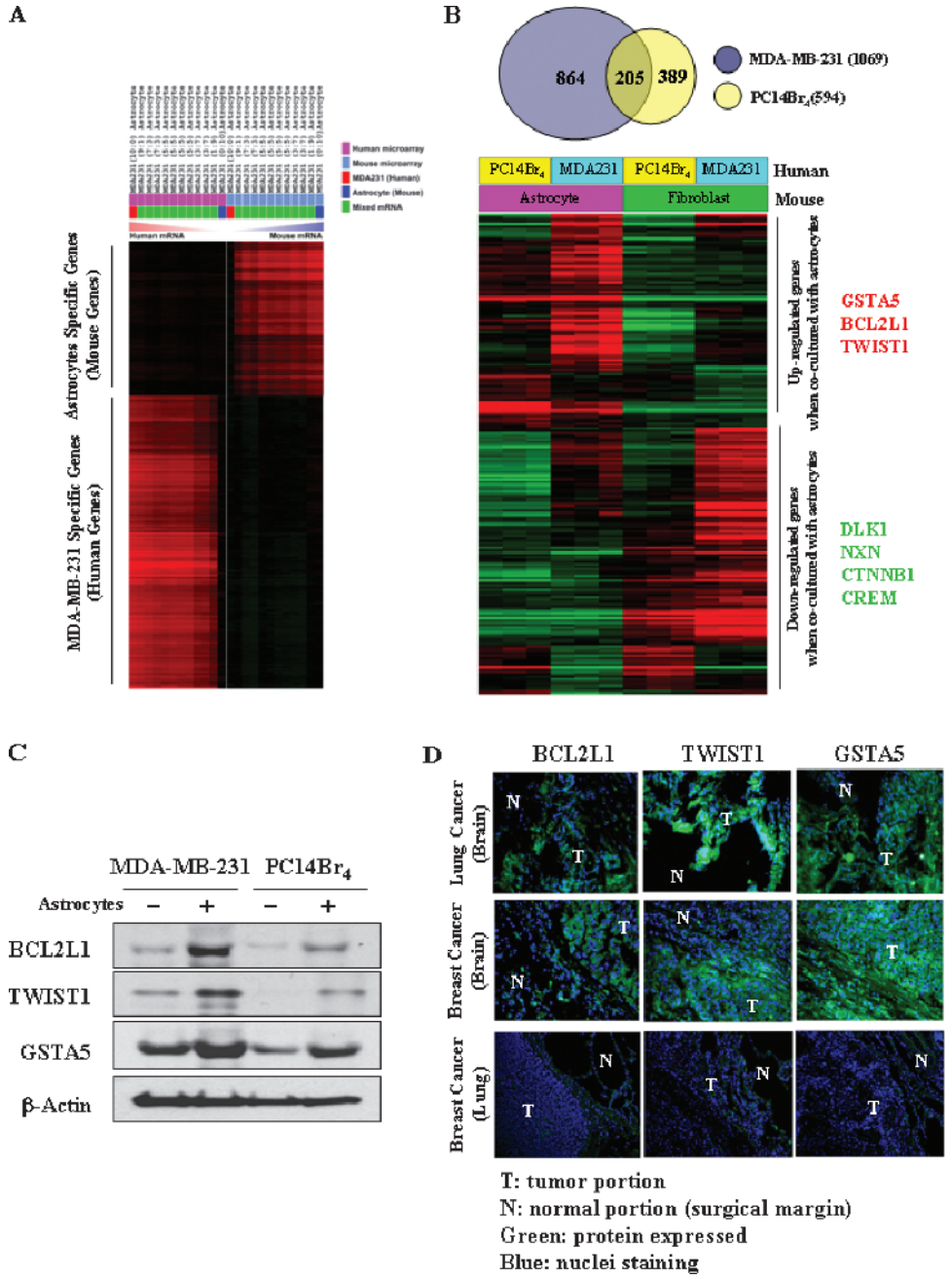

Figure 4. (A) Measured expression patterns of human and mouse genes by cross-species hybridization with human and mouse RNA microarray slides. The data are presented in matrix format in which rows represent individual gene and columns represent each hybridization event. Each cell in the matrix represents the expression level of a gene feature in an individual hybridization. The red in cells reflects measured expression levels, and intensity of color represents the magnitude of expression (log_2-transformed scale). These results confirm the specificity of the analyses. (B) Expression patterns of human genes in MDA-MB-231 and $PC14Br_4$ cocultured with murine astrocytes or 3T3 cells. We identified genes whose expression patterns were altered on interaction with astrocytes in each cell line by applying two-sample *t* tests ($P < .001$). In MDA-MB-231 and $PC14Br_4$ cells, 1069 and 594 genes, respectively, were differentially expressed. The expression of 205 genes was altered in both cell lines. Of these, several are related to antiapoptosis and cell survival. (C) Validation of microarray by Western blot analysis. Protein was extracted from MDA-MB-231 and $PC14Br_4$ cells after they were cultured alone or with or murine astrocytes. The expression of the antiapoptotic survival genes *BCL2L1*, *TWIST1*, and *GSTA* was upregulated in MDA-MB-231 and $PC14Br_4$ cells cocultured with murine astrocytes. (D) Expression of *BCL2L1*, *TWIST1*, and *GSTA5* in clinical specimen of breast cancer and lung cancer metastasis in the brain and breast cancer in the brain and lung. *BCL2L1*, *TWIST1*, and *GSTA5* were highly expressed (green) on tumor cells. Nuclei were stained with 4′,6-diamidino-2-phenylindole (blue). Tumor cells in clinical specimen of breast cancer metastases to the lung were negative for expression of these genes, whereas low expression of these genes was detected in normal alveolar epithelial cells and alveolar macrophages.

cells that were first cultured with astrocytes and then with 3T3 fibroblasts (50.3% ± 4.1% *vs* 83.3% ± 3.1%, $P < .01$). $PC14Br_4$ lung cancer cells initially cocultured with fibroblasts and in the second cycle with astrocytes also had a significant decrease in apoptotic index, but not with fibroblasts (44.4% ± 2.5% *vs* 81.0% ± 2.6%, $P < .01$). Tumor cells initially cocultured with fibroblasts and again with fibroblasts were not protected from chemotherapy (control culture 80.7 ± 5.8 *vs* 81.0 ± 2.6, $P = .896128$; Figure 5*A*). These data clearly demonstrate that increased tumor cell resistance to multiple chemotherapeutic drugs requires continuous direct contact with astrocytes.

The gene expression data from the two cycles of coculture experiments indicated that the influence of the second coculture was dominant in gene expression patterns of the cancer cells. Regardless of the first coculture condition, $PC14Br_4$ cells cocultured with astrocytes in the second cycle exhibited a distinctive gene expression signature that was detected in the first cycle culture experiments (high expression of *GSTA5*, *BCL2L1*, and *TWIST1*), whereas cancer cells cocultured with astrocytes in the first round lost the specific gene expression signatures when they were cocultured with fibroblasts in the second round (Figure 5*B*). This result parallels that of the *in vitro* chemoprotection assay and strongly indicates that the gene expression pattern in the tumor cells depended on constant contact with the astrocytes.

RNA microarray data of human and mouse genes can be accessed at the following sites: http://www.ncbi.nlm.nih.gov/geo/query/acc.cgi?token=zbwtvaeeaqsgqlk&acc=GSE19179 and http://www.ncbi.nlm.nih.gov.geo.query/acc.cgi?token=dlqntswkqsuuerm&acc=GSE26293.

Genetic Modulations of Survival Genes BCL2L1, GSTA5, *and* TWIST1 *in Tumor Cells Alter the Resistance of Tumor Cells to the Chemotherapeutic Agent in Cultures with or without Astrocytes*

Specific down-regulation of corresponding protein expression by siRNA was confirmed by Western blot analysis (Figure 6*A*). Transfection of tumor cells with siRNA targeting *BCL2L1*, *GSTA5*, and *TWIST1* alone did not affect astrocyte-mediated tumor cell protection when exposed to taxol (Figure 6*B*, *upper panel*); however, reversal of the

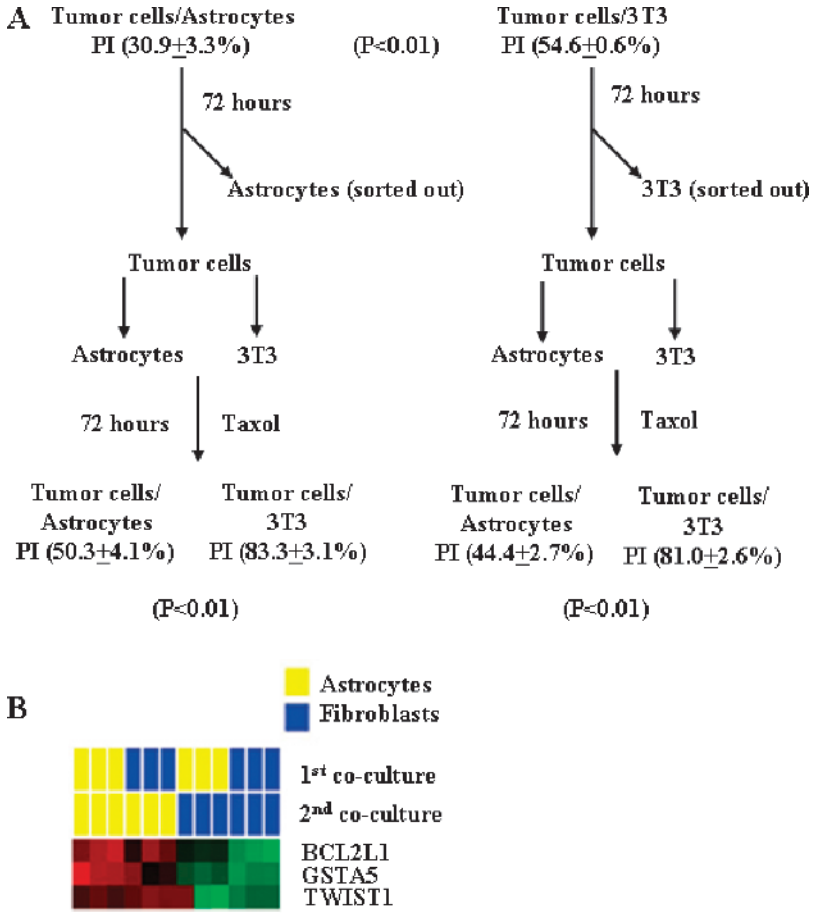

Figure 5. Chemoprotection requires constant contact with astrocytes. (A) The apoptotic index of $PC14Br_4$ cells cultured with astrocytes was 30.9% ± 3.3%, and with fibroblasts, it was 54.6% ± 0.6% ($P > .01$). Tumor cells initially cultured with astrocytes were harvested and reincubated with astrocytes or fibroblasts in the presence of taxol for another 72 hours. Tumor cells cocultured again with astrocytes maintained the relative resistance to taxol compared with tumor cells cocultured (second cycle) with fibroblasts. Tumor cells initially cultured with fibroblasts were not resistant to taxol, but if these tumor cells were then reincubated (second cycle) with astrocytes, they developed resistance compared with tumor cells cultured again with fibroblasts. (B) Gene expression of *BCL2L1*, *GSTA5*, and *TWIST1* was determined in $PC14Br_4$ cells cultured with astrocytes or fibroblasts. Similar to data shown in Figure 3, the survival genes were highly expressed in tumor cells cocultured with astrocytes but not with fibroblasts (first cycle). We harvested surviving tumor cells and cocultured them for the second cycle with either astrocytes or fibroblasts. Once again, only tumor cells cocultured with astrocytes (second cycle) expressed higher levels of *BCL2L1*, *GSTA5*, and *TWIST1*.

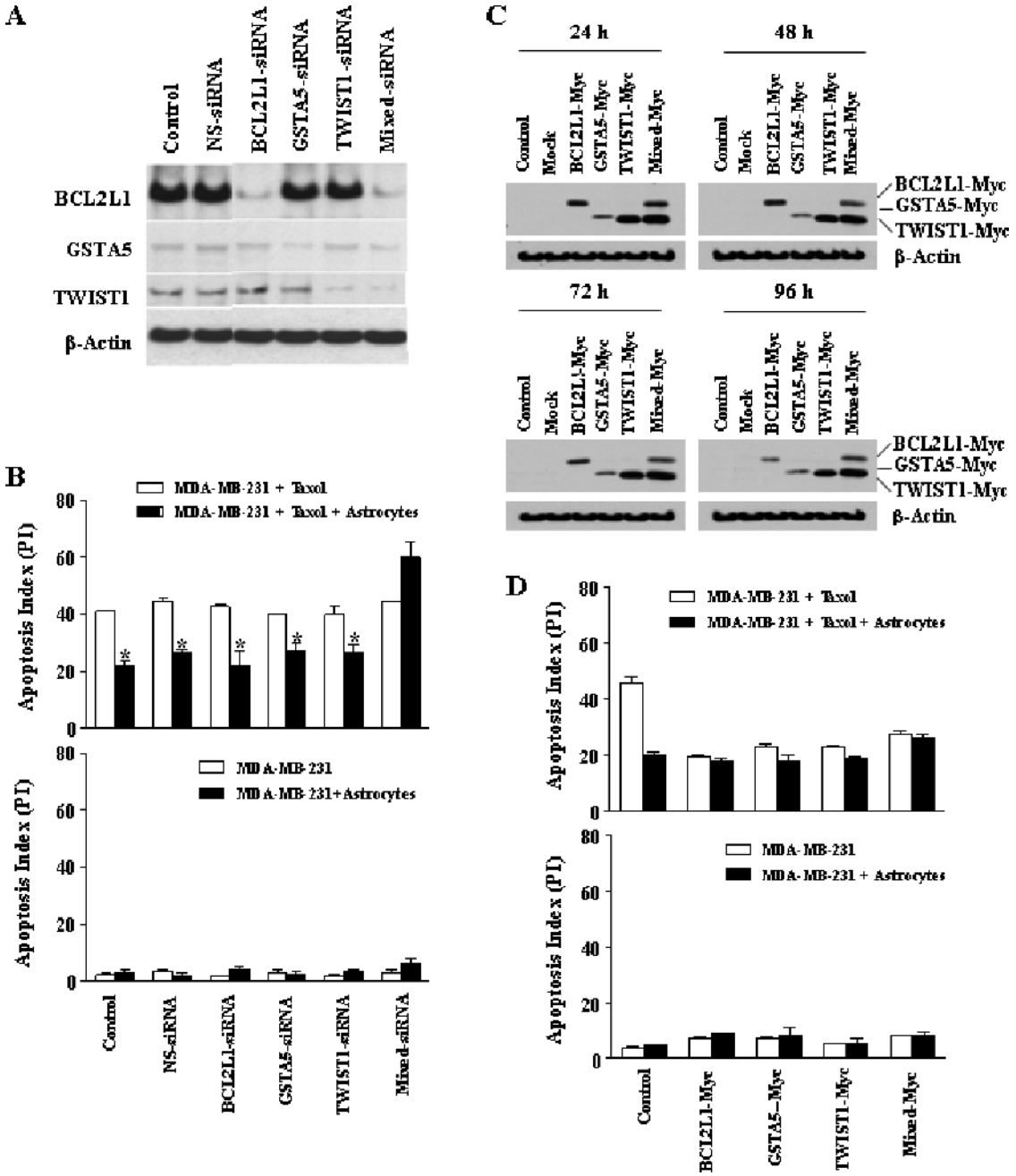

Figure 6. (A) Western blot analysis for validation of knockdown of target genes using siRNA. The results demonstrate specificity of the transfection with siRNA in the down-regulation of corresponding protein expression level. (B) Upper panel. Chemoprotection assay. Reversal of the protection by astrocytes was achieved only when all three genes were knocked down. Lower panel. Transfection of MDA-MD-231 human breast cancer cells with siRNA targeting *BCL2L1*, *GSTA5*, and *TWIST1* did not affect the apoptosis index. (C) Stable expression of *BCL2L1*, *GSTA5*, and *TWIST1* genes. Western blot analysis using anti-Myc antibody shows stable overexpression of targeted genes at the indicated time points. (D) Effects of overexpression of *BCL2L1*, *GSTA5*, and *TWIST1* genes of tumor cells on chemoprotection mediated by murine astrocytes. Overexpression of *BCL2L2*, *GSTA5*, *TWIST1* alone or all three genes increased tumor cell resistance to taxol in the absence of astrocytes (upper panel). Overexpression of single gene or pool of genes did not affect the apoptosis index of tumor cells in control cultures (lower panel). *$P < .01$.

protective effects of astrocytes for tumor cells from taxol could only be achieved when the tumor cells were transfected with siRNA targeting all three genes. Specifically, the protection from chemotherapy was still observed in cells transfected with siRNA targeting only NS, only *BCL2L1*, only *GSTA5*, or only *TWIST1* (41.3 ± 0.4 *vs* 23.1 ± 1.1, 43.4 ± 0.7 *vs* 27.1 ± 0.8, 42.6 ± 0.5 *vs* 21.0 ± 3.1, 40.3 ± 0.5 *vs* 26.5 ± 1.7, and 41.2 ± 2.3 *vs* 27.5 ± 1.7, respectively, $P < .01$). In contrast, protection from chemotherapy was reversed in cells transfected with siRNA targeting all three genes (44.9 ± 0.3 *vs* 58.5 ± 3.5, $P > .05$) (Figure 6*B*, *upper panel*). In the absence of taxol, siRNA had no effect on the apoptotic index (Figure 6*B*, *lower panel*).

In the next set of experiments, we transfected the MDA-MB-231 cells with *BCL2L1*, *GSTA5*, and *TWIST1* genes. Tumor cells stably overexpressed those genes at various time points (Figure 6*C*). Overexpression

of a single gene or pool of genes did not affect the apoptosis index of the tumor cells in the control cultures (Figure 6*D*, *lower panel*). Overexpression of *BCL2L1*, *GSTA5*, *TWIST1*, or a pool of these three genes led to resistance of tumor cells from taxol in the absence of astrocytes (19.8 ± 0.3 *vs* 18.2 ± 1.2, 23.0 ± 1.2 *vs* 18.1 ± 2.3, 23.3 ± 0.6 *vs* 19.4 ± 0.4, and 27.8 ± 1.2 *vs* 26.5 ± 1.4, respectively, $P > .05$) (Figure 6*D*, *upper panel*). Therefore, overexpression of any one gene was sufficient to induce resistance, but all three needed to be knocked down to have a protective effect.

Determination of the Role of Survival Genes BCL2L1, GSTA5, *and* TWIST1 *in AKT and MAPK Activation and the Role of AKT and MAPK Activation in the Regulation of* BCL2L1, GSTA5, *and* TWIST1 *Gene Expression*

The activation of AKT and MAPK pathways has been reported to have a functional and mechanistic relationship with *BCL2L1* [39,40], *TWIST1* [41,42], and *GSTA5* [43] genes in drug resistance, antiapoptosis, and survival of tumor cells. We therefore performed Western blot analyses for the expression of phosphorylated AKT and phosphorylated MAPK. Coculture of tumor cells with astrocytes upregulated the expression of phosphorylated AKT and phosphorylated MAPK, whereas coculture of tumor cells with 3T3 cells did not (Figure 7*A*). When we knocked down *BCL2L1* or *TWIST1*, or *GSTA5*, or all three genes, the activation of AKT or MAPK pathways was not altered (Figure 7*B*). In contrast, inhibition of AKT or MAPK phosphorylation by V/Triciribine and UO126, respectively, prevented the up-regulation of *TWIST1*, *BCL2L1*, and *GSTA5* genes (Figure 7*C*). These data clearly demonstrate that AKT and MAPK pathways are upstream of astrocyte-mediated up-regulation of expression of *BCL2L1*, *TWIST1*, and *GSTA5* genes in tumor cells.

Discussion

Our present findings raise the intriguing possibility that in addition to maintaining homeostasis [44], regulating neuronal activity to so-called "neuron-astrocyte metabolic coupling" [45], and protecting neurons from apoptosis produced by hydrogen peroxide [46], ethanol [19], and copper-catalyzed cysteine [17], astrocytes can also protect tumor cells from chemotherapeutic drugs. The murine astrocytes used in our studies expressed GFAP, the major intermediate filament protein in the central nervous system of adults [46–48]. Under a variety of conditions, these murine astrocytes protected different human tumor cells from cytotoxicity mediated by P-glycoprotein–associated and P-glycoprotein–dissociated chemotherapeutic drugs. We also demonstrated that the protection of tumor cells from chemotherapy was contact-dependent because the effect was abrogated when tumor cells and astrocytes were separated by a semipermeable membrane or when tumor cell–astrocyte cultures were treated with CBX, a specific inhibitor of GJCs [28,29]. The protection was unique to astrocytes because fibroblasts (or other tumor cells) were unable to provide protection. The protection of tumor cells by astrocytes required constant contact. Tumor cells that were first cocultured with astrocytes and then cocultured with fibroblasts were no longer protected from chemotherapy. In contrast, tumor cells initially cocultured with fibroblasts (sensitive) and then with astrocytes became more resistant to the chemotherapy. These results suggested that the protection of tumor cells from chemotherapeutic agents depended on constant interaction with astrocytes. We have previously reported that the protective effects by astrocytes are due to the sequestration of calcium from the cytoplasm of tumor cells

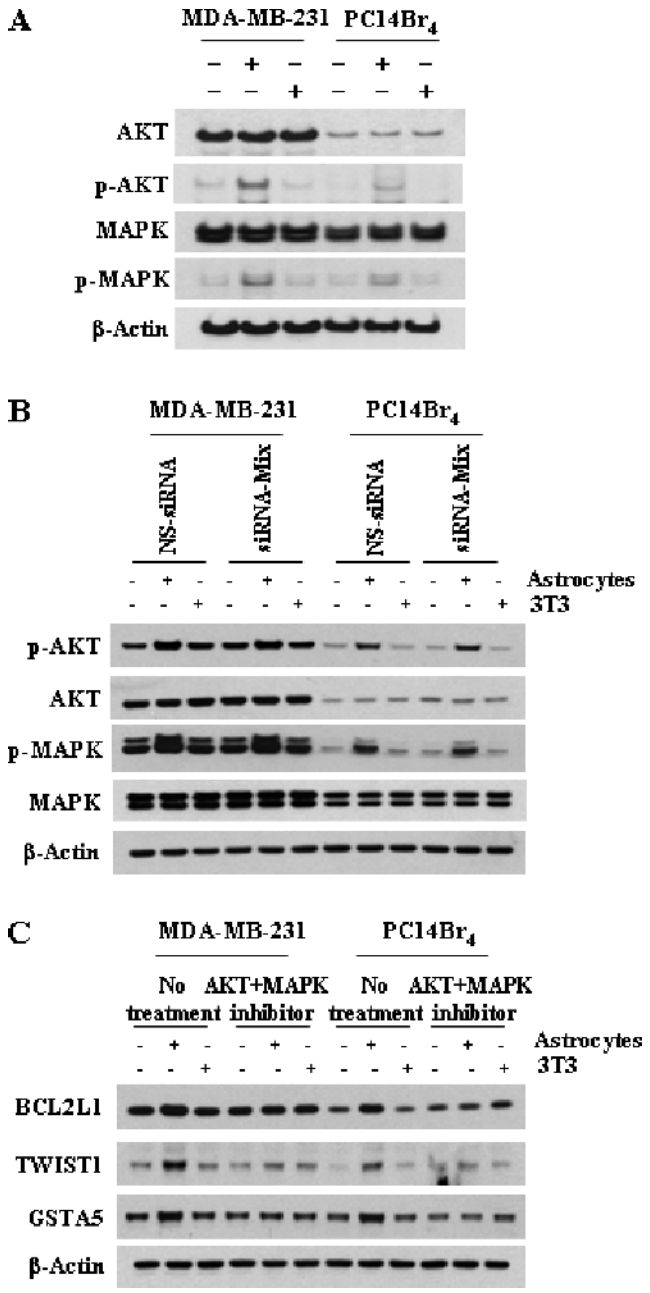

Figure 7. (A) Western blot analysis for expression of AKT/pAKT and MAPK/pMAPK in human breast cancer cells and lung cancer cells cultured alone or cocultured with astrocytes or fibroblasts. Expression of AKT and MAPK was not altered whether tumor cells were cultured alone or cocultured with astrocytes or fibroblasts. However, the expression of phosphorylated AKT or MAPK was up-regulated only in tumor cells cocultured with astrocytes. (B) Determination of the role of *BCL2L1*, *GSTA5*, and *TWIST1* genes in AKT and MAPK activation. Transfection with nonspecific (NS-siRNA) and combined siRNA (Mixed siRNA) did not affect activation of AKT and MAPK pathways. (C) Determination of the role of AKT and MAPK activation in the regulation of *BCL2L1*, *GSTA5*, and *TWIST1* gene expression. Inhibition of activation of the AKT and MAPK pathways inhibited the up-regulation of the expression of *BCL2L1*, *GSTA5* and *TWIST1* genes. All figures are representative of one experiment of three independent experiments.

[22]. Calcium has been shown to play a causal role in cell death [49]. Whereas the sequestration of calcium through GJC can explain the mechanism by which astrocytes protect tumor cells from chemotherapy, it does not rule out additional mechanisms, such as up-regulation of survival genes in tumor cells, as shown in the current study.

The direct cell-to-cell contact between astrocytes and tumor cells altered the pattern of gene expression in both tumor cells and astrocytes. The use of murine astrocytes (and murine fibroblasts as negative control) and human tumor cells (breast, lung) allowed us to identify the altered genes in the tumor cells. Among many genes, we found significant up-regulation of multiple genes that regulate cell survival. Once again, the overexpression of these genes was dependent on continuous contact between astrocytes and tumor cells. For functional validation, the expression of *BCL2L1*, *TWIST1*, and *GSTA5* was confirmed in clinical specimens of breast and lung cancer brain metastases. A study to investigate the correlation of gene expression and induction of drug resistance was performed with siRNA. The role of those genes in protection against taxol was determined by coculturing astrocytes with MDA-MB-231 cells. This protection could be reversed only when the tumor cells were transfected with mixed siRNA targeting all three genes. These data demonstrate the biologic redundancy of these survival pathways that can be used by cells to resist cytotoxic drugs leading to apoptosis. The up-regulation of phosphorylated AKT and phosphorylated MAPK subsequent to coculturing of tumor cells with astrocytes, but not with 3T3 fibroblasts, supports the conclusion that activation of these pathways leads tumor cells to resistance, antiapoptosis, and survival when exposed to chemotherapeutic agents. Knocking down the three survival genes did not prevent AKT and MAPK pathways from being activated, whereas blockade of AKT and MAPK pathway activation inhibited the up-regulation of *BCL2L1*, *TWIST1*, and *GSTA5* expression. Hence, the activation of AKT and MAPK pathways is upstream, leading to the up-regulation of expression of survival genes in tumor cells contacting astrocytes. In any case, the increased expression of *GSTA5*, *TWIST1*, and *BCL2L1* in tumor cells required constant contact with astrocytes. We base this conclusion on the data showing that the high expression of these survival genes in tumor cells was reduced once the tumor cells were transferred to cultures of fibroblasts. Immunohistochemical staining of clinical specimen of lung cancer and breast cancer metastases to the brain clearly demonstrate the expression of *GSTA5*, *TWIST1*, and *BCL2L1* genes in tumor cells but not in adjacent normal brain tissue. Collectively, these data clearly demonstrate that host cells in the organ microenvironment influence the behavior of tumor cells [19,50] and reinforce the contention that the organ microenvironment must also be taken into consideration during the design of therapy. Indeed, tumor cells are known to exploit their host for growth and survival [11], and the role of astrocytes in the induction of drug resistance of brain metastases provides a new concept for the design of therapy for the most fatal aspect of cancer.

Acknowledgments

The authors thank Walter Pagel for critical editorial review and comments and Lola López for expert assistance with the preparation of the article.

References

[1] Sawaya R, Bindal R, and Lang FF (2001). Metastatic brain tumors. In *Brain Tumors.* AH Kaye and EE Laws (Eds). Churchill-Livingstone, New York, NY. pp. 999–1026.

[2] Landis SH, Murray T, Bolden S, and Wingo PA (1998). Cancer statistics, 1998. *CA Cancer J Clin* **48**, 6–29.

[3] Norden AD, Wen PY, and Kesari S (2005). Brain metastases. *Curr Opin Neurol* **18**, 654–661.

[4] Palmieri D, Smith QR, Lockman PR, Bronder J, Gril B, Chambers AF, Weil RJ, and Steeg PS (2006). Brain metastases of breast cancer. *Am J Pathol* **26**, 139–147.

[5] Abbott N (2002). Astrocytes-endothelial interactions and blood-brain barrier permeability. *J Anat* **200**, 629–638.

[6] Lockman PR, Mittapalli RK, Taskar KS, Rudraraju V, Gril B, Bohn KA, Adkins CE, Roberts A, Thorsheim HR, Gaasch JA, et al. (2010). Heterogeneous blood-tumor barrier permeability determines drug efficacy in experimental brain metastases of breast cancer. *Clin Cancer Res* **16**, 5664–5678.

[7] Yano S, Shinohara H, Herbst RS, Kuniyasu H, Bucana CD, Ellis LM, Davis D, McConkey DJ, and Fidler IJ (2000). Expression of vascular endothelial growth factor is necessary but not sufficient for production and growth of brain metastasis. *Cancer Res* **60**, 4959–4967.

[8] Gerstner ER and Fine RL (2007). Increased permeability of the blood-brain barrier to chemotherapy in metastatic brain tumors: establishing a treatment paradigm. *J Clin Oncol* **25**, 2306–2312.

[9] Kamoun WS, Ley CD, Farrar CT, Duyverman AM, Lahdenranta J, Lacorre DA, Batchelor TT, di Tomaso E, Duda DG, Munn LL, et al. (2009). Edema control by cediranib, a vascular endothelial growth factor receptor–targeted kinase inhibitor, prolongs survival despite persistent brain tumor growth in mice. *J Clin Oncol* **27**, 1–13.

[10] Cordon-Cardo C, O'Brien JP, Boccia J, Casals D, Bertino JR, and Melamed MR (1990). Expression of the multidrug resistance gene product (P-glycoprotein) in human normal and tumor tissues. *J Histochem Cytochem* **38**, 1277–1287.

[11] Talmadge JE and Fidler IJ (2010). AACR centennial series: the biology of cancer metastasis: historical perspective. *Cancer Res* **70**, 5649–5669.

[12] Seth P and Koul N (2008). Astrocyte, the star avatar: redefined. *J Biosci* **33**, 405–421.

[13] Koehler RC, Gebremedhin D, and Harder DR (2006). Role of astrocytes in cerebrovascular regulation. *J Appl Physiol* **100**, 307–317.

[14] Iadecola C and Nedergaard M (2007). Glial regulation of the cerebral microvasculature. *Nat Neurosci* **10**, 1369–1376.

[15] Haydon PG and Carmignoto G (2006). Astrocyte control of synaptic transmission and neurovascular coupling. *Physiol Rev* **86**, 1009–1031.

[16] Nedergarrd M (1994). Direct signaling from astrocytes to neurons in cultures of mammalian brain cells. *Science* **263**, 1768–1771.

[17] Verkhratsky A and Kirchhoff F (2007). Glutamate-mediated neuronal-glial transmission. *J Anat* **210**, 651–660.

[18] Gee JR and Keller JN (2005). Astrocytes: regulation of brain homeostasis via apolipoprotein E. *Int J Biochem Cell Biol* **37**, 1145–1150.

[19] Wang XF and Cynader MS (2001). Pyruvate released by astrocytes protects neurons from copper-catalyzed cystein neurotoxocity. *J Neurosci* **21**, 3322–3331.

[20] Faulkner JR, Herrmann JE, Woo MJ, Tansey KE, Doan NB, and Sofroniew MV (2004). Reactive astrocytes protect tissue and preserve function after spinal cord injury. *J Neurosci* **24**, 2143–2155.

[21] Trendelenburg G and Dirnagl U (2005). Neuroprotective role of astrocytes in cerebral ischemia: focus on ischemic preconditioning. *Glia* **51**, 307–320.

[22] Lin Q, Balasubramanian K, Fan D, Kim SJ, Guo L, Wang H, Bar-Eli M, Aldape KD, and Fidler IJ (2010). Reactive astrocytes protect melanoma cells from chemotherapy by sequestering intracellular calcium through gap junction channels. *Neoplasia* **12**, 748–754.

[23] Schackert G and Fidler IJ (1988). Site-specific metastasis of mouse melanomas and a fibrosarcoma in the brain or meninges of syngeneic animals. *Cancer Res* **48**, 3478–3484.

[24] Kim SJ, Uehara H, Yazici S, Busby JE, Nakamura T, He J, Maya M, Logothetis C, Mathew P, Wang X, et al. (2006). Targeting platelet-derived growth factor receptor on endothelial cells of multidrug-resistant prostate cancer. *J Natl Cancer Inst* **98**, 783–793.

[25] Langley RR, Fan D, Tsan RZ, Rebhun R, He J, Kim SJ, and Fidler IJ (2004). Activation of the platelet-derived growth factor-receptor enhances survival of murine bone endothelial cells. *Cancer Res* **64**, 3727–3730.

[26] Dull T, Zufferey R, Kelly M, Mandel RJ, Nguyen M, Trono D, and Naldini L (1998). A third-generation lentivirus vector with a conditional packaging system. *J Virol* **72**, 8463–8471.

[27] Galipeau J, Li H, Paquin A, Sicilia F, Karpati G, and Nalbantoglu J (1999). Vesicular stomatitis virus G pseudotyped retrovector mediates effective *in vivo* suicide gene delivery in experimental brain cancer. *Cancer Res* **59**, 2384–2394.

[28] Goldberg GS, Moreno AP, Bechberger JF, Hearn SS, Shivers RR, MacPhee DJ, Zhang YC, and Naus CC (1996). Evidence that disruption of connexin particle arrangements in gap junction plaques is associated with inhibition of gap junctional communication by a glycyrrhetinic acid derivative. *Exp Cell Res* **222**, 48–53.

[29] Guan X, Wilson S, Schlender KK, and Ruch RJ (1996). Gap-junction disassembly and connexin 43 dephosphorylation induced by 18 β-glycyrrhetinic acid. *Mol Carcinog* **16**, 157–164.

[30] Zamai L, Canonico B, Luchetti F, Ferri P, Melloni E, Guidotti L, Cappellini A, Cutroneo G, Vitale M, and Papa S (2001). Supravital exposure to propidium iodide identifies apoptosis on adherent cells. *Cytometry* **44**, 57–64.

[31] Fan D, Bucana CD, O'Brian CA, Zwelling LA, Seid C, and Fidler IJ (1990). Enhancement of tumor cell sensitivity to adriamycin by presentation of the drug in phosphatidylcholine-phosphatidylserine liposomes. *Cancer Res* **50**, 3619–3626.

[32] Bucana CD, Hoyer LC, Schroit AJ, and Fidler IJ (1983). Ultrastructural studies of the interaction between liposome-activated human blood monocytes and allogeneic tumor cells *in vitro*. *Am J Pathol* **112**, 101–111.

[33] Wade MH, Trosko JE, and Schindler M (1986). A fluorescence photobleaching assay of gap junction-mediated communication between human cells. *Science* **232**, 525–528.

[34] Lin JH, Weigel H, Cotrina ML, Liu S, Bueno E, Hansen AJ, Hansen TW, Goldman S, and Nedergaard M (1998). Gap-junction–mediated propagation and amplification of cell injury. *Nat Neurosci* **1**, 494–500.

[35] Fonseca PC, Nihei OK, Savine W, Spray DC, and Alves LA (2006). Flow cytometry analysis of gap junction–mediated cell-cell communication: advantages and pitfalls. *Cytometry* **69A**, 487–493.

[36] Trosko JE and Ruch RJ (2002). Gap junctions as targets for cancer chemoprevention and chemotherapy. *Curr Drug Targets* **3**, 465–482.

[37] Bolstad BM, Irizarry RA, Astrand M, and Speed TP (2003). A comparison of normalization methods for high density oligonucleotide array data based on variance and bias. *Bioinformatics* **19**, 185–193.

[38] Krysko DV, Leybaert L, Vandenabeele P, and D'Herde K (2005). Gap junctions and the propagation of cell survival and cell death signals. *Apoptosis* **10**, 459–469.

[39] Qian J, Zou Y, Rahman JS, Lu B, and Massion PP (2009). Synergy between phosphatidylinositol 3-kinase/Akt pathway and Bcl-xL in the control of apoptosis in adenocarcinoma cells of the lung. *Mol Cancer Ther* **8**, 101–109.

[40] Yu YL, Chiang YJ, Chen YC, Papetti M, Juo CG, Skoultchi AI, and Yen JJ (2005). MAPK-mediated phosphorylation of GATA-1 promotes Bcl-xL expression and cell survival. *J Biol Chem* **19**, 29533–29542.

[41] Cheng GZ, Chan J, Wang Q, Zhang W, Sun CD, and Wang LH (2007). Twist transcriptionally upregulates AKT2 in breast cancer cells leading to increased migration, invasion, and resistance to taxol. *Cancer Res* **67**, 1979–1987.

[42] Zhang X, Wang Q, Ling MT, Wong YC, Leung SC, and Wang X (2007). Anti-apoptotic role of *TWIST* and its association with Akt pathway in mediating taxol resistance in nasopharyngeal carcinoma cells. *Int J Cancer* **120**, 1891–1898.

[43] Kazi S and Ellis EM (2002). Expression of rat liver glutathione-*S*-transferase *GSTA5* in cell lines provides increased resistance to alkylating agents and toxic aldehydes. *Chem Biol Interact* **20**, 121–135.

[44] Volterra A and Meldolesi J (2005). Astrocytes, from brain glue to communication elements: the revolution continues. *Nat Rev Neurosci* **6**, 626–640.

[45] Kasischke KA, Vishwasrao HD, Fisher PJ, Zipfel WR, and Webb WW (2004). Neural activity triggers neuronal oxidative metabolism followed by astrocytic glycolysis. *Science* **305**, 99–103.

[46] Desagher S, Glowinski J, and Premont J (1996). Astrocytes protect neurons from hydrogen peroxide toxicity. *J Neurosci* **16**, 2553–2562.

[47] Sofroniew MV (2005). Reactive astrocytes in neural repair and protection. *Neuroscientist* **11**, 400–407.

[48] Pekny M and Nilsson M (2005). Astrocyte activation and reactive gliosis. *Glia* **50**, 427–434.

[49] Roderick HL and Cook SJ (2008). Ca^{2+} signaling checkpoints in cancer: remodeling Ca^{2+} for cancer cell proliferation and survival. *Nat Rev Cancer* **8**, 361–375.

[50] Gupta GP and Massagué J (2006). Cancer metastasis: building a framework. *Cell* **127**, 679–695.